Surpporting information

In-situ engineered ZnS-FeS heterostructures in N-doping carbon nanocages accelerating polysulfides redox kinetics for lithium sulfur batteries

Wenda Li, Zhijiang Gong, Xiujuan Yan, Dezhu Wang, Jing Liu, Xiaosong Guo, Zhonghua Zhang* and Guicun Li*

College of Materials Science and Engineering, Qingdao University of Science and Technology, Qingdao 266042, China

E-mail: zhangzh@qust.edu.cn; guicunli@qust.edu.cn

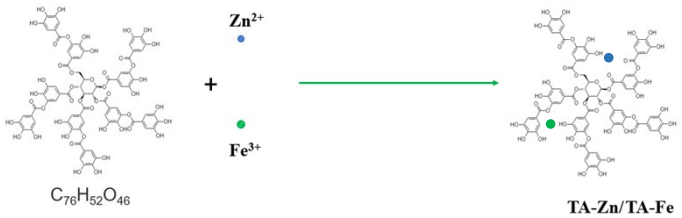

Fig. S1. The schemical reaction between mental ion and TA.

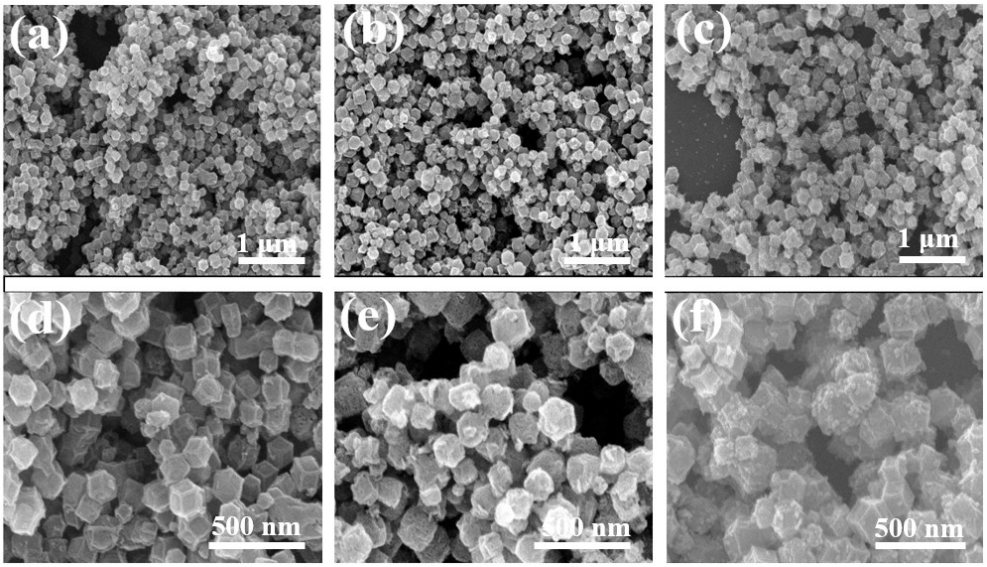

Fig. S2. The SEM images of Fe/ZIF-8 with different Fe:Zn ratio (a)-(d) 1:2; (b)-(e) 1:1; (c)-(f) 2:1.

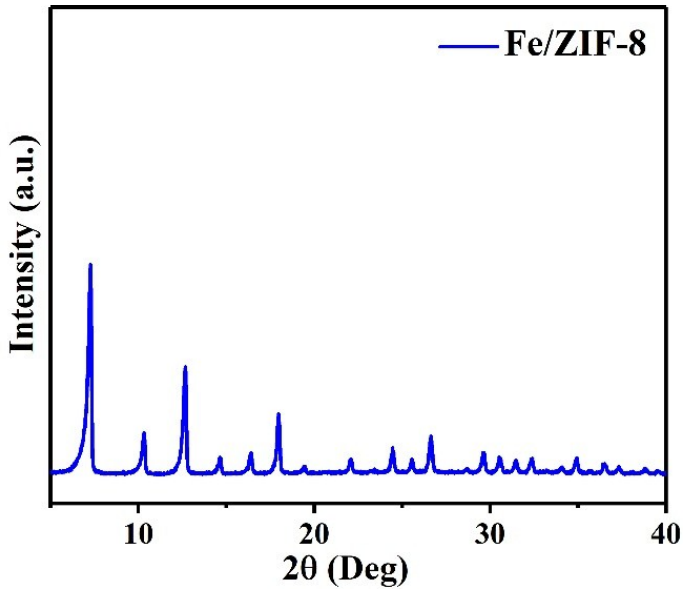

Fig. S3. The XRD patrons of Fe/ZIF-8 samples.

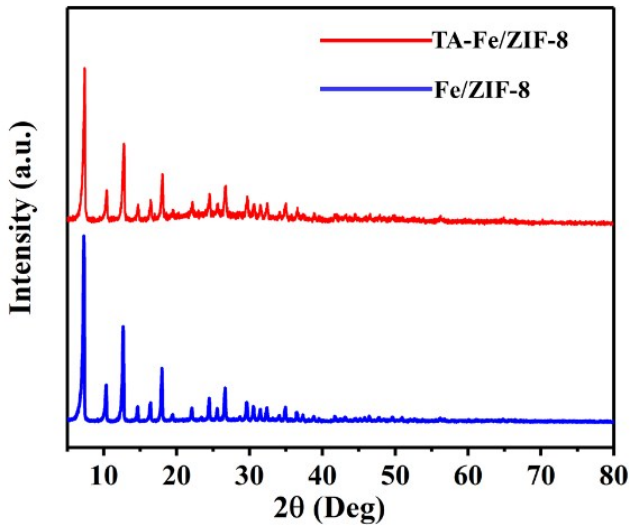

Fig. S4. The XRD patrons of Fe/ZIF-8 and TA-ZIF-8 nanocages.

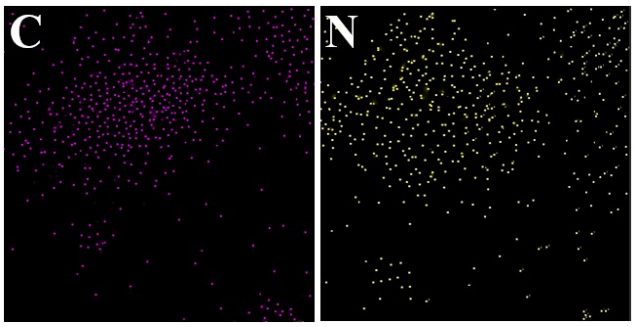

Fig. S5. The EDS mapping images of ZnS-FeS/NC samples for C and N elements

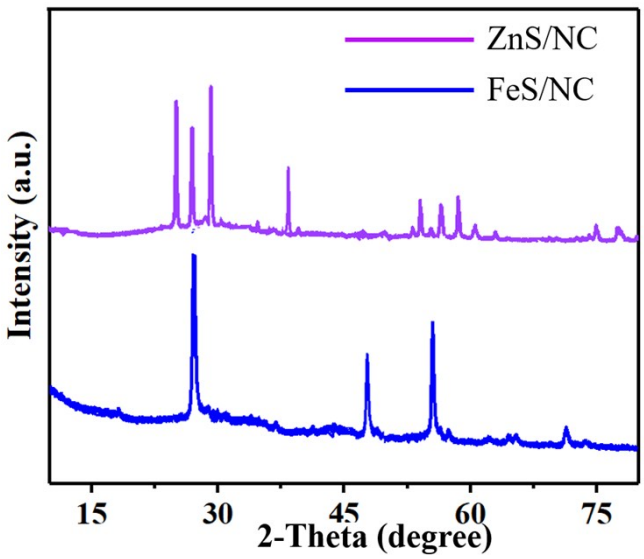

Fig. S6. The XRD patterns of ZnS/NC and FeS/NC composites.

Table S1. Co and Fe content in ZnS-FeS@NC sample analyzed by ICP technique.

Sample	Zn (wt.%)	Fe (wt.%)
ZnS-FeS@NC	20.3	9.6

Table S2. C and N content in ZnS-FeS@NC sample analyzed by EA technique.

Sample	C (wt.%)	N (wt.%)
ZnS-FeS@NC	44.2	6.4

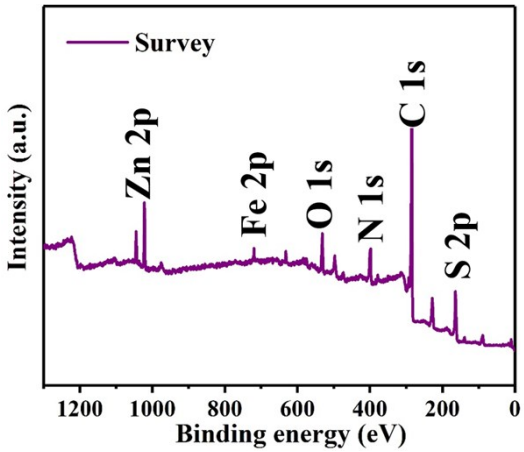

Fig. S7. The XPS survey of FeS-ZnS/NC samples.

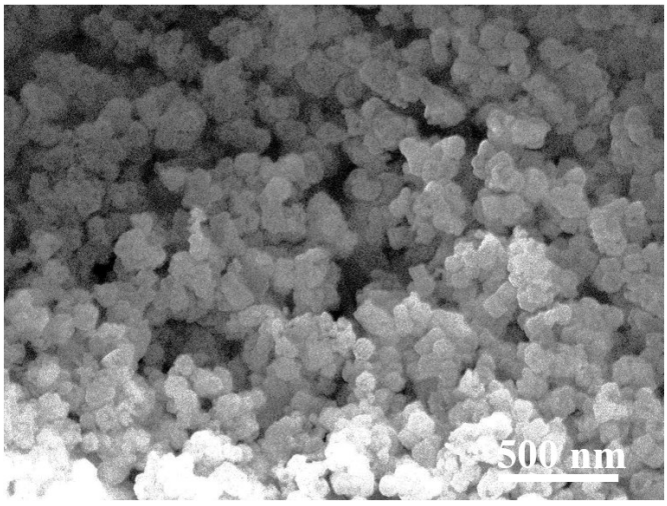

Fig. S8. The SEM images of S@ZnS-FeS/NC composite.

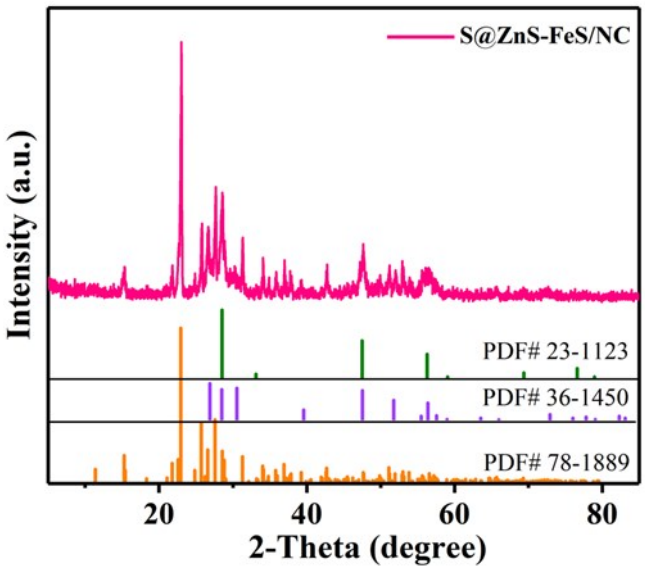

Fig. S9. The XRD pattern of S@ZnS-FeS/NC composite.

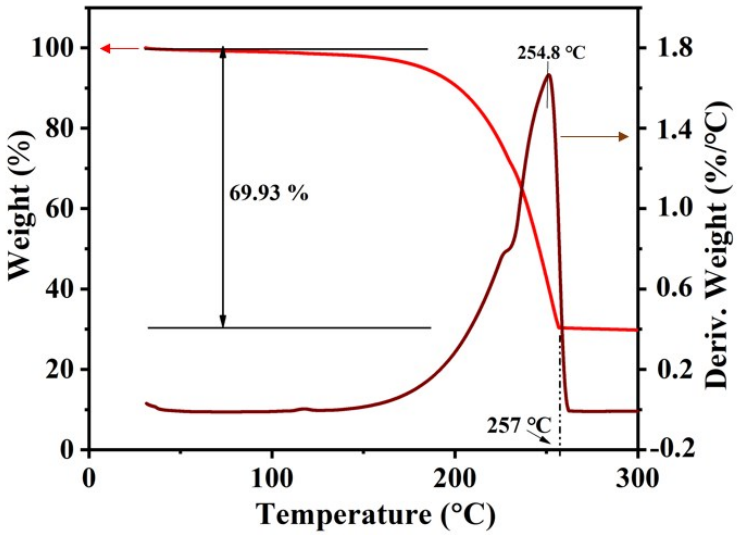

Fig. S10. The TGA and DSC curves of the S@ZnS-FeS@NC composite.

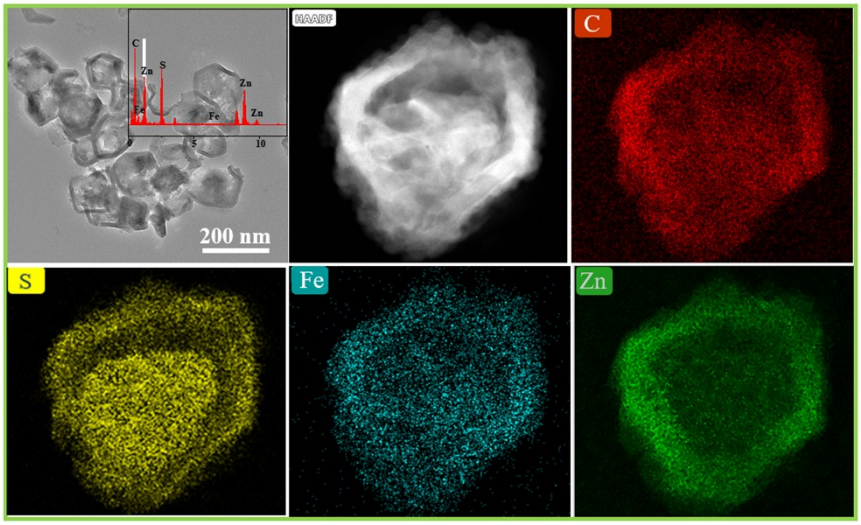

Fig. S11. TEM image of the S@ZnS-FeS@NC and the corresponding EDS elemental mapping images.

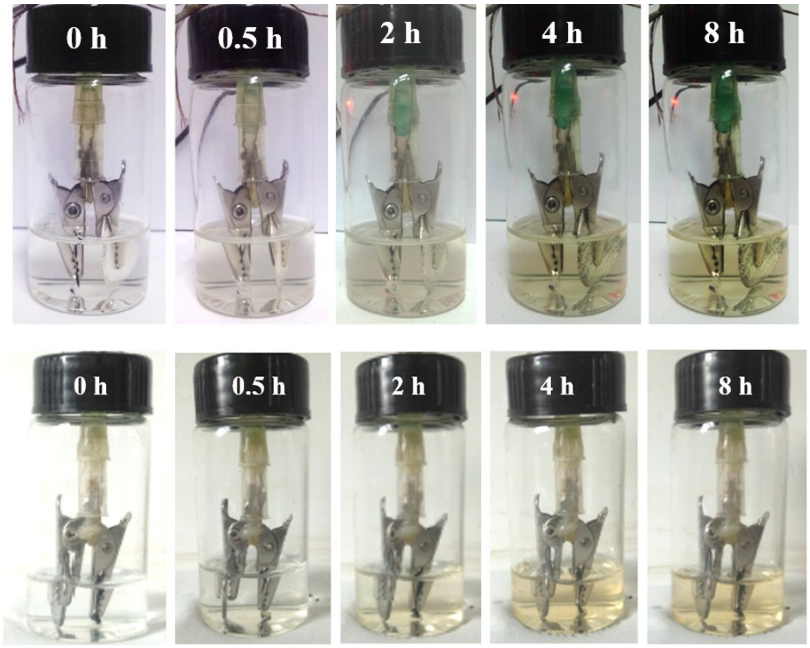

Fig. S12. Digital photos of the visual Li-S cell with S@ZnS/NC cathode and S@FeS/NC at different time.

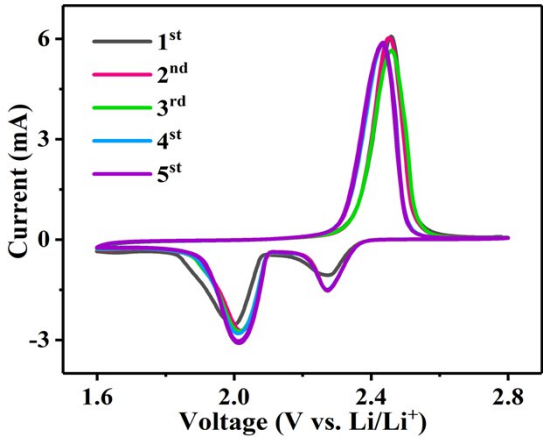

Fig. S13. The CV curves of the S@ZnS-FeS/NC cathode for the first five cycles at a scan rate of 0.1 mV s^{-1}

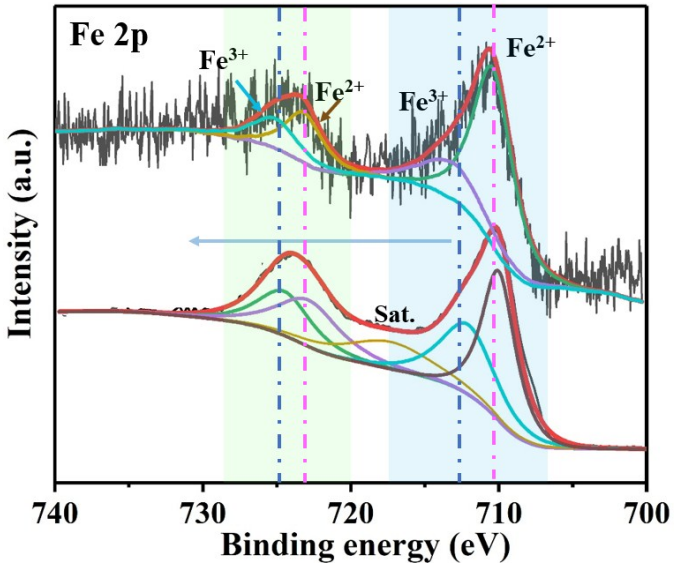

Fig. S14. Fe2p XPS spectrum of ZnS-FeS/NC and ZnS-FeS/NC+Li_2S_6.

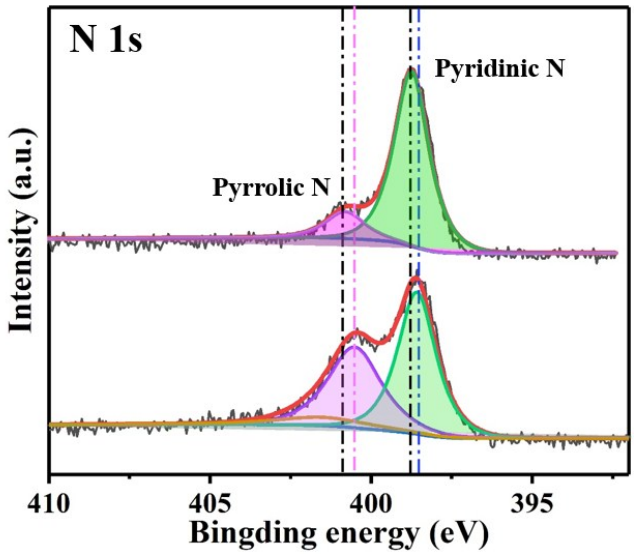

Fig. S15. N1s XPS spectrum of ZnS-FeS/NC and ZnS-FeS/NC+Li_2S_6.

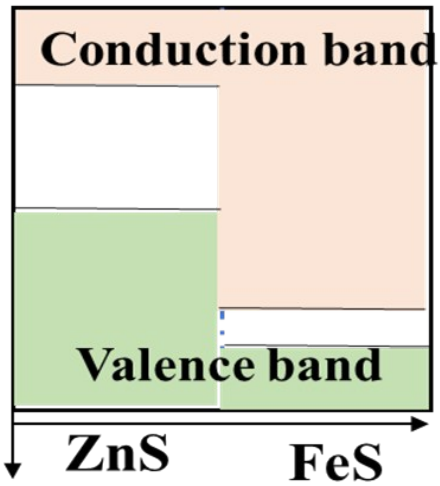

Fig. S16. The band alignment of the ZnS and FeS.

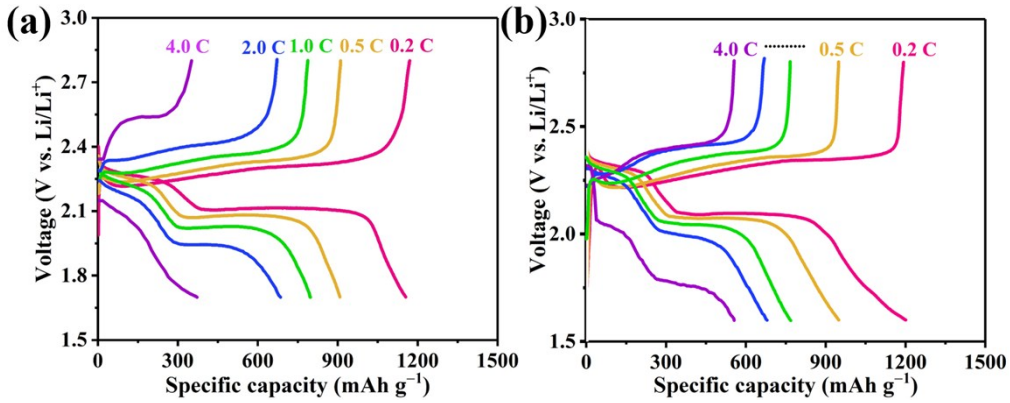

Fig. S17. The charge and discharge profiles at different current densities of S@ZnS/NC and S@FeS/NC composites cathode.

Table S3. Performance comparison between S@ZnS-FeS/NC and sulfur electrodes based on metal sulfides in recent publications.

1	S@ZnS-FeS/NC	738 mA h g^{-1} 4.0 C	**This work**
2	S/CoS_2	580 mA h g^{-1} 2.0 C	Ref.[1]
3	S/CuS	568 mAh g^{-1} at 3.0 C	Ref.[2]
4	NiS@C-HS	718 mAh g^{-1} at 4.0 C	Ref.[3]
5	rGO–VS_2/S	616 mAh g^{-1} 3.0 C	Ref.[4]
6	MnS nanocrystal decorated N/S codoped graphene	572 mAh g^{-1} 4.0 C	Ref.[5]
7	S/AHCNS-SnS_2	717.6 mAh g^{-1} 2.0 C	Ref.[6]

8	Co_3S_4@S	617 mAh g^{-1} 4.0 C	Ref.[7]
9	NbS_2@S@I-Doped Graphene	603 mAh g^{-1} 5.0 C	Ref.[8]
10	C@WS_2/S	448 mAh g^{-1} 3.0 C	Ref.[9]

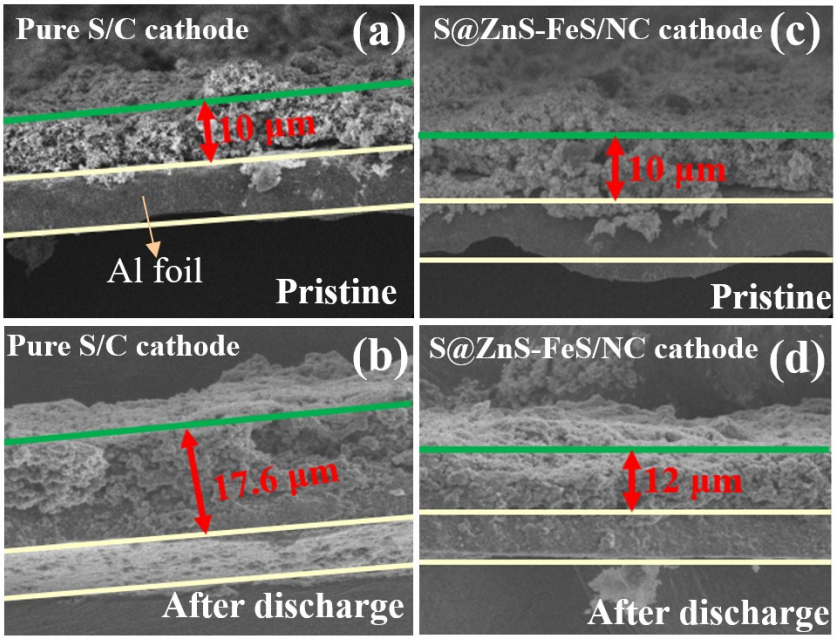

Fig. S18. The pristine and after discharge cross-sectional SEM image of the sulfur/carbon (a)-(b) and S@ZnS-FeS/NC (c)-(d) cathodes with low sulfur loading.

Supporting Reference

1. J. Zhou, N. Lin, W. l. Cai, C. Guo, K. Zhang, J. Zhou, Y. Zhu and Y. Qian, *Electrochim. Acta*, 2016, **218**, 243-251.
2. H. Li, L. Sun, Y. Zhao, T. Tan and Y. Zhang, *Appl. Surface Sci.*, 2019, **466**, 309-319.
3. C. Ye, L. Zhang, C. Guo, D. Li, A. Vasileff, H. Wang and S.-Z. Qiao, *Adv. Funct. Mater.*, 2017, **27,** 1702524.
4. Z. Cheng, Z. Xiao, H. Pan, S. Wang and R. Wang, *Adv. Energy Mater.*, 2018, **8,** 1702337.
5. Z. Li, R. Xu, S. Deng, X. Su, W. Wu, S. Liu and M. Wu, *Appl. Surface Sci.*, 2018, **433**, 10-15.
6. X. Li, L. Chu, Y. Wang and L. Pan, *Mater. Sci. Eng.: B*, 2016, **205**, 46-54.
7. J. Pu, Z. Shen, J. Zheng, W. Wu, C. Zhu, Q. Zhou, H. Zhang and F. Pan, *Nano Energy*, 2017, **37**, 7-14.
8. Z. Xiao, Z. Yang, L. Zhang, H. Pan and R. Wang, *ACS Nano*, 2017, **11**, 8488-8498.

9. T. Lei, W. Chen, J. Huang, C. Yan, H. Sun, C. Wang, W. Zhang, Y. Li and J. Xiong, *Adv. Energy Mater.*, 2017, **7,** 1601843.